



Effect of thermoplastic impregnation on the mechanical behaviour of textile reinforcement for concrete

Kira Heins¹ · Sophie Lesker¹ · Julius Pütz¹ · Michael Hüntemann¹ · Thomas Gries¹

Received: 25 October 2022 / Accepted: 8 February 2023

Published online: 25 February 2023

© The Author(s) 2023

Abstract

In recent decades, textile reinforced concrete (TRC) has become increasingly important, both in research and the construction industry. It is a resource-efficient material alternative to conventional, steel reinforced concrete due to the use of non-corroding high-performance textile reinforcements and the resulting material savings. Typically, thermoset polymer materials are used as impregnation for the textile reinforcement to improve the mechanical behaviour. However, due to their chemically crosslinking behaviour, these materials prevent subsequent product-specific shaping of the reinforcement. The use of thermoplastic impregnation materials shows potential to allow shaping by utilizing the thermal forming behaviour, provided that the resulting properties of the reinforcement system in terms of mechanical performance are not inferior to those of the already available impregnations. In this study, four impregnation systems are investigated on AR-glass textiles with regard to their effect on the mechanical behaviour of the reinforcement and classified in comparison to the current benchmark epoxy and styrene butadiene rubber (SBR) by conducting single yarn tensile tests and supporting microscopy analysis. The thermoplastic impregnation increased the tensile strength of the AR glass fibre to values in the range of around 1200 MPa with a low coating content to 1500 MPa with a high coating content. A strong dependence of the impregnation efficiency on the impregnation composition, in this case the solid content of the dispersion, was demonstrated as a result of pore formation. In conclusion, thermoplastic impregnation materials achieve strengths comparable to those of commonly used materials.

Article Highlights

- Thermoplastic impregnations show comparable mechanical performance to conventional thermoset impregnations
- Efficient thermoplastic impregnations will influence the application breakthrough of textile-reinforced concrete
- Solids content and material of impregnation play an essential role in mechanical utilization degree of reinforcement

Keywords TRC · Technical textiles · Impregnation · Concrete composites · Coating · Textile reinforcement

✉ Kira Heins, Kira.heins@ita.rwth-aachen.de | ¹Institut Für Textiltechnik, RWTH Aachen University, Otto-Blumenthal-Straße 1, 52074 Aachen, Germany.



1 Introduction

In many industries, the demand for sustainable, resource efficient and high performance materials and processes has increased. In many cases the lightweight design of products by application of composites with a fibre based reinforcement has hence grown in interest. In construction the use of composite materials is already common praxis as for the past century the most commonly used material was concrete reinforced by steel grids. Within this composite, the concrete carries compressive loads applied to the structural element, whereas the steel reinforcement carries applied tensile loads [1]. One major challenge is the corrosion potential of the steel reinforcement which can result into spalling of the concrete and influences the service life of the structure. For that reason, a comparatively thick concrete cover is applied [2]. Counteracting these disadvantages is the application of fibre based reinforcement materials. These fibre based reinforcements can be implemented in a variety of forms such as short-fibre reinforcement or two dimensional grid structures made from either rovings or rebars similar to conventional steel reinforcement grids [2]. Textile reinforced concrete (TRC) describes a construction material wherein the conventional steel reinforcements are replaced by technical textiles made of non-metallic fibre materials [3]. The most commonly used fibre materials are alkali-resistant AR glass fibres and carbon fibres. Here AR glass fibres are the less expensive alternative but lag behind carbon fibres in terms of mechanical performance and durability [4, 5]. The non-corrosive nature of the fibre materials when in contact with air allows a reduction of the concrete cover and the production of resource-efficient thin-walled high-performance elements [6]. On the other hand, the resistance of the fibre material in the alkaline concrete environment plays a significant role in the durability of the components. The alkaline environment can cause damage to the reinforcement and thus a loss of strength of the reinforcement and a reduction in the load-bearing capacity of the concrete element. Assessments under accelerated ageing conditions indicate that no strength loss is to be expected for carbon reinforcements, while non-impregnated AR glass reinforcements may experience a strength loss of up to 40% within 50 years when exposed to outdoor weathering in a cool temperate climate. [7]. In conclusion, the essential requirements for the textile reinforcement aside from high mechanical performance are good alkaline resistance and bond behaviour with the surrounding cementitious matrix. Good operability and drapeability as well as penetrability with the concrete matrix must be ensured [1, 8].

The efficiency of load bearing capacity by the reinforcement depends on the tensile strength and orientation of the filaments, the type of fibres, the fibre diameter, the fibre volume fraction [1, 9, 10]. Biaxial reinforced non-crimp warp knitted fabrics fulfil many of these requirements. Within the textile, rovings with a defined spacing are oriented at 90° to each other and connected by stitching yarns. The stitch width and type determine both the drapeability of the textile and the grid opening [1, 9, 11]. In addition, the stitch type affects the cross-sectional shape of the rovings. While a tricot shows relatively flat elliptical structures, a pillar type stitching results in compacted, round cross-sections. These shape differences influence the extent of bonding to the matrix and maximum tensile strength of the reinforcement [1, 9, 11].

Typically, the textile reinforcements are impregnated with a polymeric or mineral impregnating material after the textile manufacturing process to increase the overall bond strength and durability in concrete as well as allow easy processing [2, 7, 12]. Non-impregnated textiles usually fail due to pull-out failure. As the rovings consist of large number of individual filaments with only small gussets the comparatively coarse concrete matrix material cannot penetrate the roving. This causes load transmission to occur to the outer filaments by means of an adhesive bond whereas the inner filaments contribute to the load bearing only by frictional load transfer [2, 13, 14]. As a result, the high strength of the roving is not utilized to its full potential [2, 15]. The polymer impregnation material on the other hand penetrates the inner gussets and creates an adhesive bond between the individual filaments [2, 15]. In this way, the load transfer and the utilization of the high-performance properties are improved [1, 2]. The impregnation usually occurs in-line with the textile production and is followed by immediate curing of the polymer [12]. For use as an impregnation material, the polymer system must show a high penetration capacity into the internal gussets of the roving, a high cohesive strength in the cured state and a high durability and temperature resistance. For this reason, solvent or water-based dispersions or reactive polymer systems are usually used [2, 16]. The most commonly used impregnating materials—epoxy resins or styrene-butadiene rubbers (SBR)—are chemically crosslinking materials. This results in an increased mechanical performance and bond behaviour but at the expense of drapeability and hence reduced design flexibility [1, 17]. An alternative to thermoset materials are thermoplastic polymers. In thermoplastics, the polymer molecule chains are oriented (semi-crystalline) or non-oriented in a physical network without forming a chemical crosslink. This allows a cyclic repetition of melting and solidification processes and thus a simplified shaping and preparation

of reinforcement cages [18]. The advantages of the thermoplastic as a matrix material are the shorter cycle times during production, the flexibility in the design of structural elements and the improved recycling behaviour [19]. Disadvantages of a thermoplastic matrix material are the lower achievable fibre volume fraction compared to reactive resins due to the often high viscosity and low penetration into the filament bundle, especially in melt systems, as well as the occurrence of instability when the glass transition temperature is exceeded [18]. Despite these seemingly critical disadvantages, thermoplastic fibre-reinforced plastics (FRP) are used in high-performance industries, e.g. aerospace and automotive, but also in construction. The most common thermoplastics for use in construction are polypropylene (PP), thermoplastic polyesters, polyamides, polyetheretherketone (PEEK) and polyethersulfone (PES). Typical thermoplastic products are glass or carbon fibre reinforced pultruded rebars, where the thermoplastic allows the realisation of stirrups, glass/PP composite panels for ceiling and wall elements and bridge ceiling panels or thin-shell roof systems [18].

In this study, preliminary investigations on the applicability of thermoplastic impregnations for non-crimp textile reinforcements are carried out. The thermoplastic material will allow reshaping of the reinforcement to realise a product- and application-specific reinforcement geometry at any later time under the supply of thermal energy. For this purpose, the efficiency of the impregnations in terms of increasing the mechanical performance of the textile reinforcement must first be investigated. Likewise, with regard to a later application, a comparison is to be made with materials already in use.

2 Methodology

The following subchapters explain the materials and methods used in the study. The subchapter material describes the type of roving, the textile geometry and the impregnation material utilised for the experimental studies. Under

the aspect of method, both the impregnation and curing process as well as the test procedures are explained.

2.1 Materials

In this work, AR glass rovings of 1200 tex are processed on a BIASTRONIC® CO, a high-performance knitting machine with weft insertion in line with the stitch course, from KARL MAYER BIASTRONIC (KARL MAYER Technische Textilien GmbH, Chemnitz, Germany), to produce a biaxial non-crimp warp knitted fabric. The maximum tensile stress of the un-processed rovings is greater than 1000 MPa according to manufacturer's datasheet. The warp and weft rovings are connected by way of a counterlaid tricot binding to realise an open grid structure. The warp and weft rovings are introduced to the machine with a centre-to-centre distance of two adjacent rovings of 16.9 mm, resulting in a grid opening of 15 mm. During production, two 1200 tex rovings are joined together so that each tension element in the textile reaches a total of 2400 tex. This results in a load-bearing cross-section of 0.89 mm^2 per tension element, or $60 \times 0.89 \text{ mm}^2 = 53.4 \text{ mm}^2/\text{m}$ of textile reinforcement. The impregnation materials used are an epoxy resin and a styrene butadiene rubber to form the benchmark. The thermoplastic impregnation materials used are a material based on polystyrene and one based on polyacrylate in the form of water-based dispersions. For both thermoplastic materials, dispersions with a solids content of around 50% and 25% are considered. The impregnation systems are summarized in Table 1.

The textile is impregnated using an immersion bath impregnation system (cf. Figure 1). Here, the textile is immersed under constant tension in an immersion bath with the impregnation material. The excess material is then squeezed off by a pair of squeezing rollers. The impregnation is cured in a two-stage oven. In the case of the water-based dispersions, the water contained is evaporated at $80 \text{ }^\circ\text{C}$ in the first oven. This is followed by consolidation and film formation at $150\text{--}160 \text{ }^\circ\text{C}$, depending on the material used.

Table 1 Impregnation materials used

Polymer	Type of material	Solid content	Identification
–	–	–	Non-impregnated
Epoxy resin	Thermoset polymer	–	EP
Aqueous styrene butadiene rubber dispersion	Rubber	50%	SBR
Aqueous polyacrylate dispersion	Thermoplastic polymer	25%	Acrylate 50
		50%	Acrylate 25
Aqueous polystyrene dispersion	Thermoplastic polymer	25%	Styrene 50
		50%	Styrene 25

Fig. 1 Schematic representation of the impregnation process with immersion bath

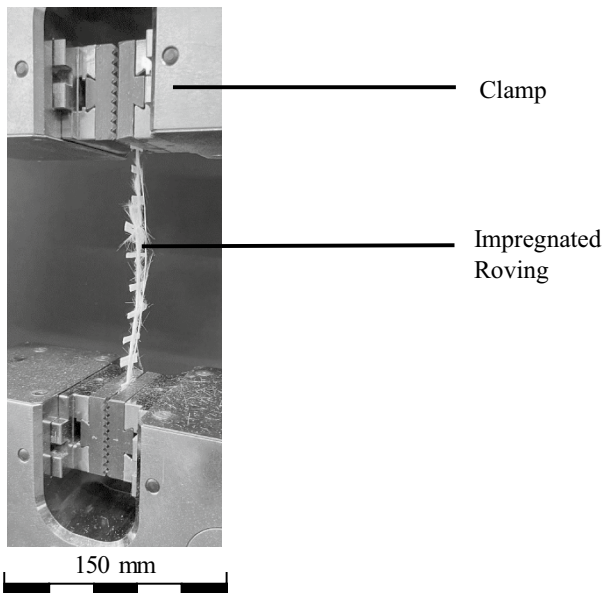
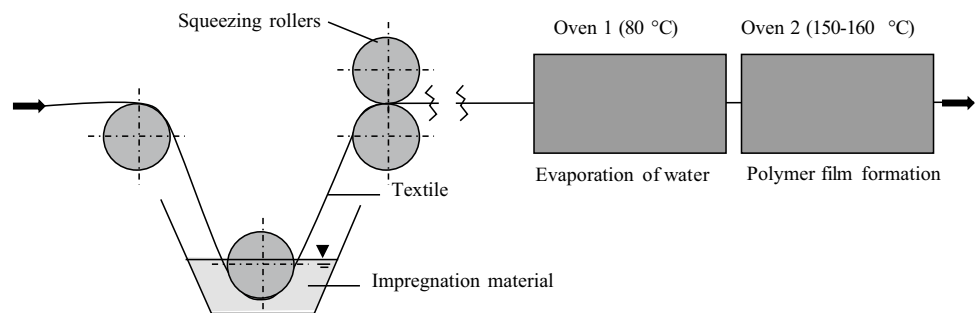


Fig. 2 Test setup of the yarn tension test on the separated yarn

2.2 Roving tensile tests on the roving separated from the textile

After impregnation individual rovings are separated from the textile. In accordance with the DIN EN ISO 9163 standard ten samples per test series are prepared with a free test length of 150 mm [20]. The clamping areas of the specimens are reinforced by cardboard elements to increase the clamping area and to reduce damage to the specimen due to clamping pressure. The tensile tests on the separated yarns are carried out with a tensile testing machine in accordance with DIN EN ISO 9163 (cf. Figure 2). For this purpose, after applying a pre-load of 0.5 cN/tex, the specimen is loaded in tension at a test speed of 10 mm/min up to a force drop of 90%.

2.3 Tensile tests on textile strip

Since the effects caused by the cross-connection of the rovings in the textile are lost in tensile tests on the

separated rovings, additional tensile tests are carried out on the textile strip. For comparability, samples of a free test length of 150 mm are utilised. Cardboard elements are used in the clamping area to improve the clamping behaviour. According to ASTM D 6637-01 [21] the specimens are prepared in a way that five rovings run in the longitudinal direction. The outermost roving on the right and left respectively are cut so that effectively three rovings are tested. The test is performed on a tensile testing machine at a test speed of 10 mm/min up to a force drop of 90%.

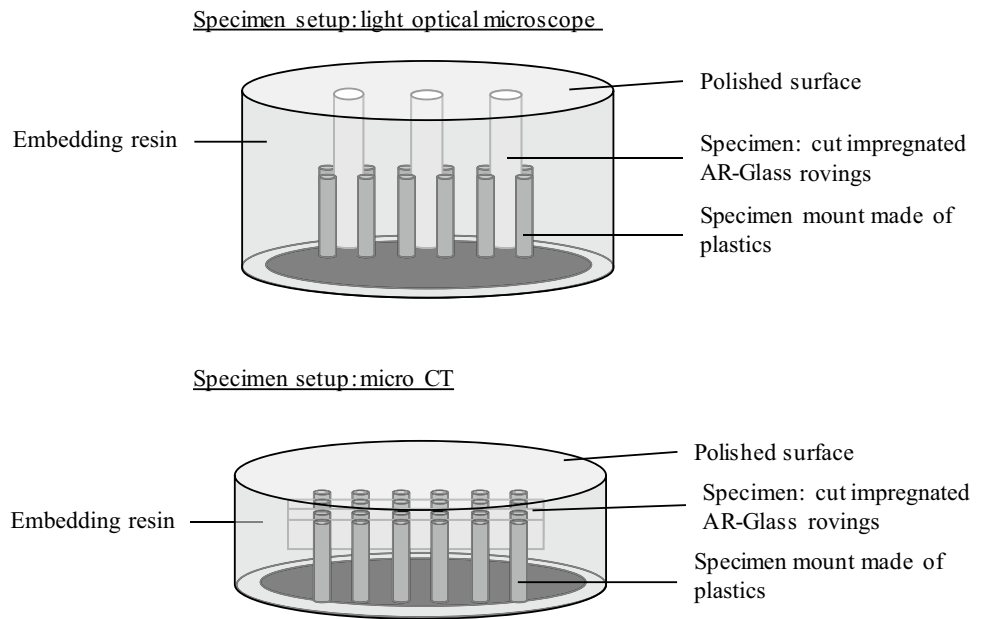
2.4 Optical analysis

The mechanical examinations are supported by optical analysis. First, light microscope images of the impregnated roving cross-section are taken. For this purpose, roving samples with a length of 12 mm are vertically set into a plastic mount. The mount is subsequently placed into a silicone mould. The clear, epoxy based embedding resin is cast into the mould and cured for 24 h. The surface of the specimen is then ground and polished. The microscopy images are taken with a light microscope DM4000M, (Leica Microsystems GmbH, Wetzlar, Germany) under reflected light with 100× and 200× magnification. CT images are taken with a CT Alpha (ProCon X-Ray GmbH, Sarstedt, Germany) at 100 kV, 100µA with a 1 mm copper filter. The scan time at a resolution of 8.5 µm is two hours. For the CT scans, samples of the roving are inserted horizontally into a specimen holder at a length of 20 mm. This is embedded in a resin in the same way as above. Figure 3 Shows the specimen setup for the light microscopy (top) and the CT images (bottom).

3 Results and discussion

The tensile test on the yarn separated from the textile allows a statement about both the mode of failure and the maximum strength. When considering the results, the maximum strengths achieved by the impregnated yarns are first compared with those of a non-impregnated reference. This is followed by a comparison of the impregnated

Fig. 3 Schematic illustration of the specimen setup for imaging analysis



samples with each other. In addition to looking at the mean values, taking into account the standard deviations of the test series, an analysis of the statistical significance is carried out using a paired t-test with a significance level of $\alpha = 5\%$.

Figure 4 shows the typical curves determined for the test series. It can be clearly seen that, in addition to the maximum tensile strength, the course of the force–elongation curves is also significantly influenced. The force–elongation curve of a non-impregnated AR glass fibre roving is linear at first, flattens out and drops off with a smooth curve after reaching the maximum tensile strength. Impregnated specimens show a different curve. After a linear increase until the maximum tensile strength is reached, a gradual drop in strength can be seen. These differences

in fracture behaviour can be explained by looking at the individual tensile elements in the roving. In a non-impregnated roving, the individual filaments fail successively. The associated drop in strength is small. In impregnated rovings, there is an adhesive bond between the individual filaments. The individual filaments bonded together in this way fail together. In case of low penetration depth of the roving or low solid content of the dispersion, the adhesive bond does not form between all single filaments, but forms individual firmly bonded sections. These sections in turn fail successively. The drop in strength is clearly noticeable and leads to a gradual drop. The smaller the penetration depth or the solids content of the dispersion, the more individual bonded sections are formed and the more steps the stress–strain curve shows in the failure.

Fig. 4 Typical stress–strain curves of the yarn tensile tests for all test series

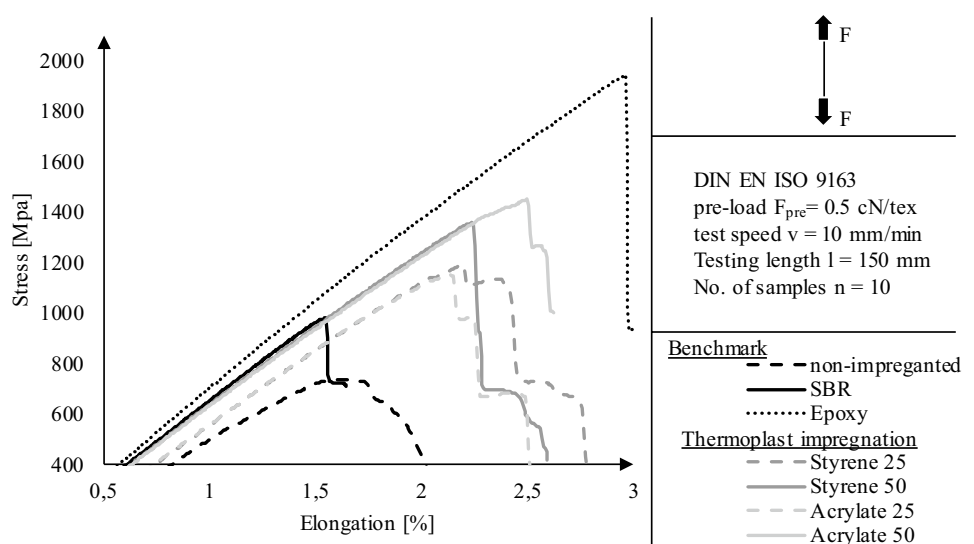


Figure 5 shows the mean values and standard deviations of the test series. Here the stress values are related to the cumulative cross sectional area of the individual AR-Glass-Filaments in the roving as they are the main load carrying elements. It can clearly be seen an increase in force for impregnated rovings in comparison to non-impregnated rovings, as expected by [1, 2]. The Benchmark achieves maximum tensile strengths of around 1160 MPa to 1520 MPa for SBR and epoxy impregnations, respectively. For the impregnations with the thermoplastic materials, strengths of 1207 MPa at a dispersion solids content of 25% and 1362 MPa at a solids content of 50% are achieved for the styrene-based impregnations. In the case of the acrylate-based impregnation, a 25% solids content in the dispersion leads to a strength of 1196 MPa, while a 50% solids content leads to a maximum strength of 1280 MPa. The values are summarised in Table 2.

The statistical evaluation determined a statistically significant difference between the pairings styrene 25-styrene 50, styrene 25-EP, styrene 50-SBR, acrylate 25-EP and acrylate 50-EP. This proves that both the chemical composition of the impregnating polymer and the solid content of the dispersion exert an influence on the efficiency of impregnation. The classification of thermoplastic materials in relation to the benchmark shows that dispersions with a lower solids content of 25% should be placed at the lower limit, i.e. at the level of SBR, while dispersions with a higher solids content tend to the upper limit, i.e. at the level of epoxy resin impregnations. In comparison to non-impregnated AR-Glass rovings, whose maximum tensile strength amounts to 900 MPa a minimum increase of 29% (SBR) and a maximum increase of 76% (EP) could be measured.

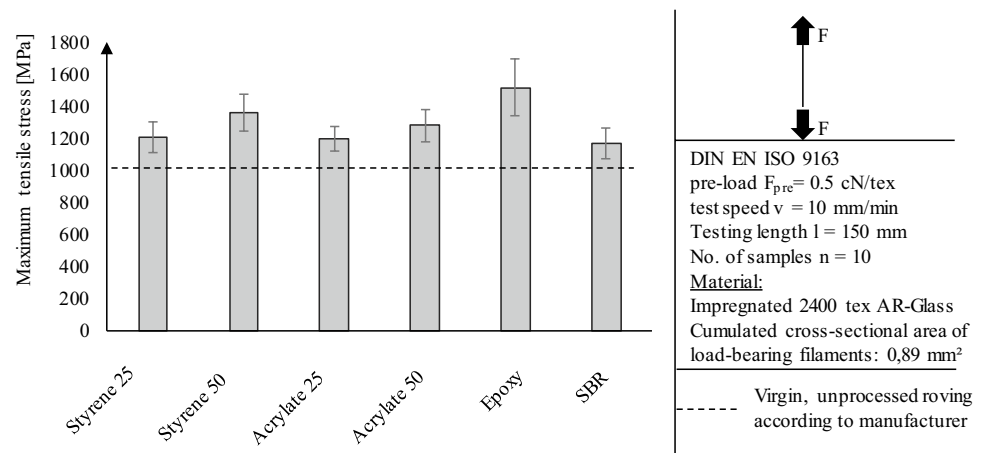
The difference in efficiency between impregnations with higher solid content values and lower solid content values can be attributed to the impregnation process as well as to the impregnation itself. Within the impregnation

Table 2 Values of Average maximum tensile stress and Standard deviation of separated rovings

Test series	Average maximum tensile stress [MPa]	Standard deviation [MPa]
EP	1518	175
SBR	1166	96
Acrylate 50	1280	101
Acrylate 25	1197	75
Styrene 50	1362	115
Styrene 25	1207	92

process, after dipping into the dispersion any excess material is removed. At the same time the squeezing rollers assist in pressuring the dispersion into inner gussets of the roving. After that, the impregnation is first dried under evaporation of the water contents and then consolidated at elevated temperature. In case of lower solid content in the dispersion most of the gusset volume is filled by the solvent, in this case the water. The large particle size of the polymer solid compared to the fluidity of the water promotes an arrangement of the polymer in the outer areas of the roving, while the squeezing pressure presses the water into the inner gussets. In conclusion, this leads to a larger remaining pore volume after the evaporation of the water. As a result, the adhesive connection between the impregnation and the individual filaments is less uniform. Subsequently the load transfer between the individual filaments is less effective. This is supported by the results from CT-scans and microscopy images. Figure 6 shows the micrographs on the cross-sectional area of the impregnated rovings. The individual glass filaments, the interface between the impregnation and the embedding resin can be clearly identified. The rovings individually compose a cross sectional area of 1 mm² in an elliptical shape. It can be found that for dispersions containing only

Fig. 5 Results of the yarn tension test: maximum tensile stress and standard deviation



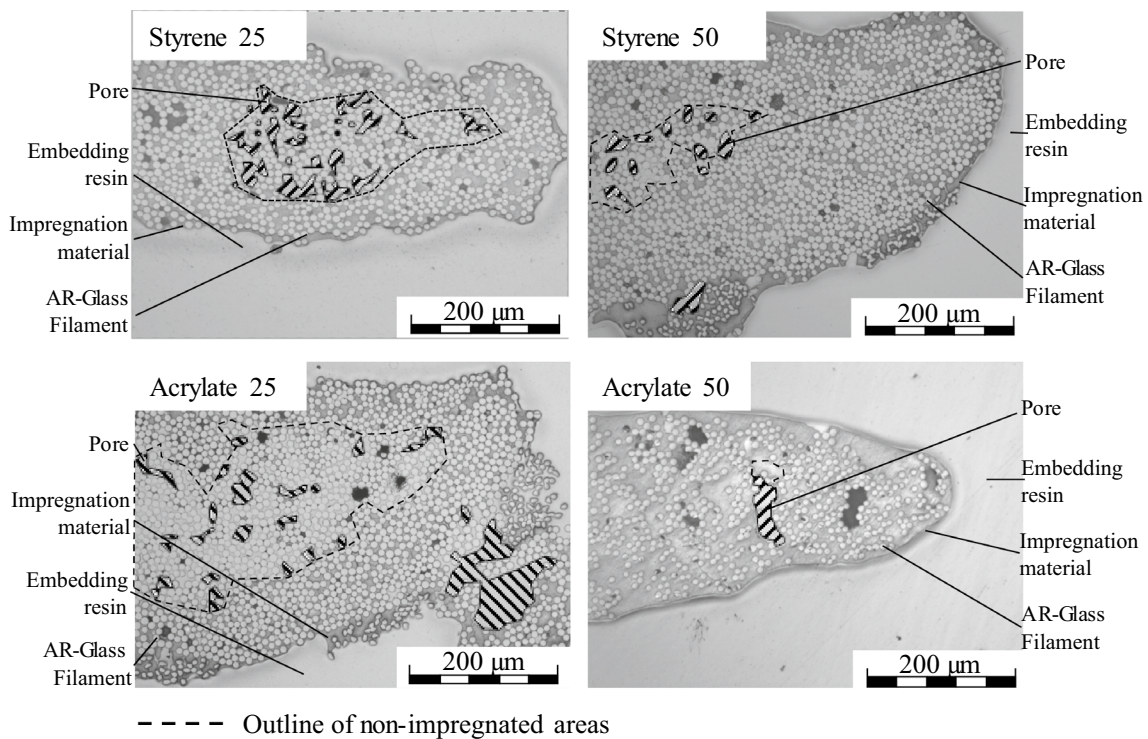


Fig. 6 Microscopy images of the cross-section for thermoplastic impregnated rovings

25% of solid content the impregnation only penetrates the gussets up to a depth of 200 μm leaving the inner core non-impregnated.

Figure 7 shows the comparison of the CT images of the four thermoplastic impregnation systems. Here, too, the images of the series with a 25% solids content in the dispersion show a higher number and length of pores per sectional image. This indicates that the pore galleries continued over long distances along the longitudinal axis of

the roving. In addition, it is clear that the pore courses form individual adhesive composites, closed in themselves, with subsets of the individual segments in the roving. Between these subsets, there is no adhesive bond, or only in places. This supports the theory that the high water content in the dispersions prevents complete consolidation.

In conclusion, due to the reduced solid content in the dispersion the roving is not fully penetrated by the polymer material hence only solidifying the connection

Fig. 7 CT images of thermo-plastic impregnated rovings in five sectional planes

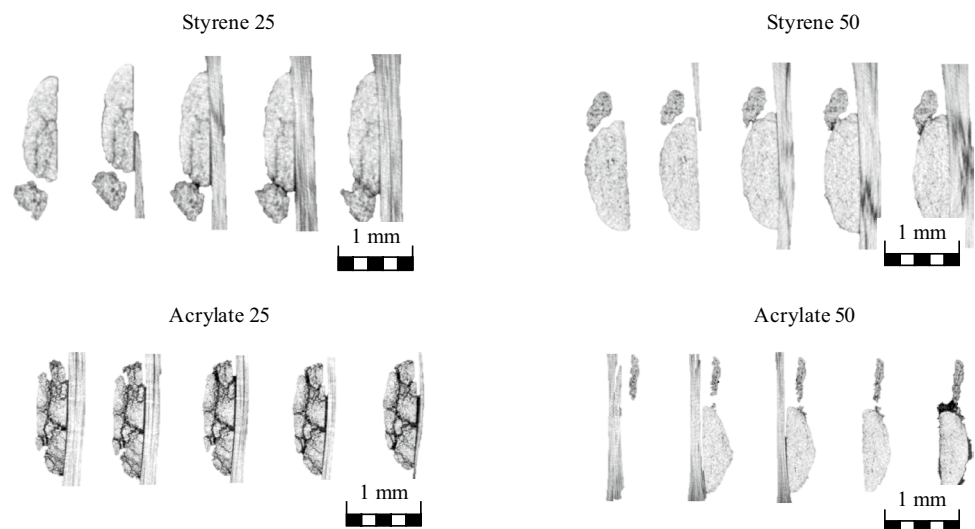
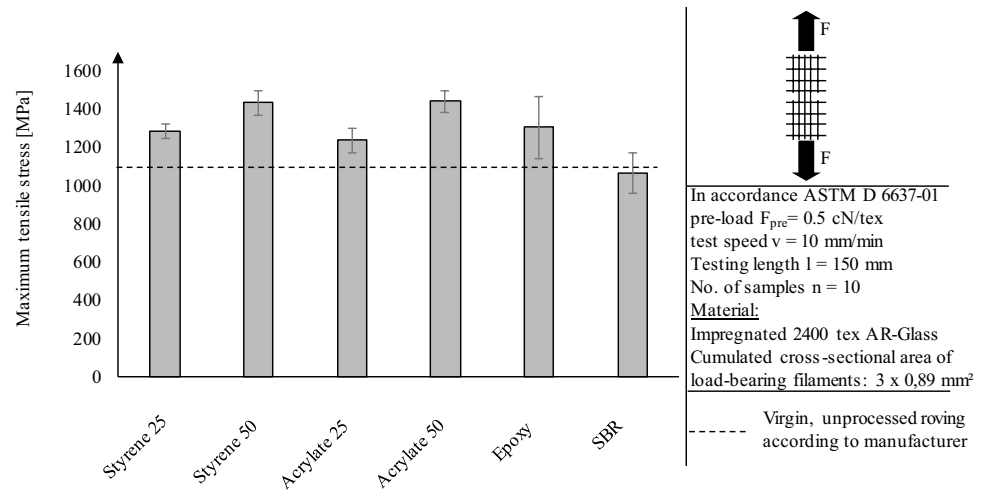


Fig. 8 Results of the tug tests on the textile strip: maximum tensile stress and standard deviation



between certain subsections of individual filaments. This leads to an increased tensile strength in comparison to non-impregnated rovings. Yet in comparison to fully impregnated rovings, i.e. with 50% dispersion, it the missing connection between the subsections prevents an effective load transfer and hence leads to a lower maximum force and a failure mode of multiple drops as seen in Fig. 3.

Figure 8 graphically represents the maximum tensile stress of the textile strip determined in the tensile tests with the values summarised in Table 3. The benchmark epoxy resin reaches a maximum strength of around 1300 MPa, the benchmark SBR amounts to 1063 MPa. In comparison, a 25% dispersion of polystyrene achieves strengths of 1284 MPa, while the 50% dispersion even reaches values of 1431 MPa. For acrylate impregnation, the values of 1235 MPa and 1438 MPa for the 25% and 50% dispersion are in comparable orders of magnitude.

The high standard deviation in the series impregnated with epoxy resin is striking here and makes statistical classification in relation to the upper limit of the industry benchmark difficult. At a significance level of $\alpha = 0.05$, only a statistically significant difference of all series to the impregnation with SBR as well as a statistically significant difference between the 50% dispersions and the 25% dispersions could be detected.

In comparison with the pure yarn tensile tests, an increase in strength is also evident, especially for the thermoplastic impregnated materials. With a 25% polystyrene coating, this is 7%, while with the 50% dispersion, the strength determined is 5% higher. For the polyacrylate impregnation, the values are 2.9% and 22% for the 25% dispersion and the 50% dispersion, respectively. This increase in strength can be explained by the presence of the weft rovings transverse to the loading direction.

Table 3 Values of Average maximum tensile stress and Standard deviation of textile strips

Test series	Average maximum tensile stress [MPa]	Standard deviation [MPa]
EP	1305	162
SBR	1063	104
Acrylate 50	1438	58
Acrylate 25	1235	67
Styrene 50	1431	66
Styrene 25	1284	40

In addition to the uniform clamping of the rovings, this connection allows force transmission to the three load-bearing tension elements.

4 Conclusion

In this study, preliminary tests were conducted to provide an initial assessment of the suitability of thermoplastic impregnations for textile reinforcement in concrete in comparison to the industrial benchmark. The impregnation of the textile reinforcements is essential to improve the efficiency of the load transfer within the roving and thus the potential utilisation of the high performance fibre material. The currently used thermoset materials cannot be moulded after the curing process. However, this significantly complicates the subsequent handling in the manufacturing process. In this study, it was demonstrated that thermoplastic impregnation materials achieve maximum tensile strengths comparable to those of the benchmark materials ranking in orders of 1200 MPa–1438 MPa. In

addition, a direct and measurable dependence between the solids content of the dispersion and the resulting strength gain of the impregnated textile could be demonstrated. Prior to the introduction of the material into building practice, further investigations must be carried out, in particular with regard to the behaviour after alkaline conditioning as occurs in the concrete environment, and to the performance development under elevated temperature, in order to demonstrate the functional safety. In addition to the material-related investigations, investigations must also be carried out in connection with the production technology, e.g. the behaviour after forming. Finally, at the composite level, statements must be made on the temperature behaviour and the bond of the concrete matrix.

Acknowledgements The authors would like to thank the German Federal Ministry of Economic Affairs and Climate Action for funding the research project as the part of the german-vietnamese joint project TRCel "Development and application of thermoplastic textile reinforcement for prefabricated TRC building elements" (FKZ KK5055916CD1).

Author contributions All authors contributed to the study conception and design. Material preparation, data collection and analysis were performed by KH, SL, MH and JP. The manuscript draft was first written by KH and reviewed by all authors. The final manuscript was approved by all authors.

Funding Open Access funding enabled and organized by Projekt DEAL. This work was supported by funding by the German Federal Ministry of Economic Affairs and Climate Action for funding the research project as the part of the german-vietnamese joint project TRCel "Development and application of thermoplastic textile reinforcement for prefabricated TRC building elements" (FKZ KK5055916CD1).

Data availability The datasets generated during and/or analyzed during the current study are available from the corresponding author on reasonable request.

Declarations

Conflict of interest The authors declare they have no financial interests that are related to the work submitted for publication.

Open Access This article is licensed under a Creative Commons Attribution 4.0 International License, which permits use, sharing, adaptation, distribution and reproduction in any medium or format, as long as you give appropriate credit to the original author(s) and the source, provide a link to the Creative Commons licence, and indicate if changes were made. The images or other third party material in this article are included in the article's Creative Commons licence, unless indicated otherwise in a credit line to the material. If material is not included in the article's Creative Commons licence and your intended use is not permitted by statutory regulation or exceeds the permitted use, you will need to obtain permission directly from the copyright holder. To view a copy of this licence, visit <http://creativecommons.org/licenses/by/4.0/>.

References

1. Peled A, Bentur A, Mobasher B (2017) Textile reinforced Concrete. CRC Press, Boca Ranton
2. Friese D, Scheurer M, Cherif C, Gries T (2022) Textile reinforcement structures for concrete construction applications—a review. *J Compos Mater.* <https://doi.org/10.1177/00219983221127181>
3. Scheerer S (2015) Was ist Textilbeton? *Beton und Stahlbetonbau* 110(S1):4–7. <https://doi.org/10.1002/best.201400104>
4. Kimm M (2020) Resource-efficient Design and Design for Recycling of Fibre-reinforced Composites in the Construction Industry; PhD Dissertation, 2020. RWTH Aachen University, Aachen
5. Cherif C (2016) Textile Materials for Lightweight Constructions. *Technol Methods Mater Proper.* <https://doi.org/10.1007/978-3-662-46341-3>
6. Hegger J, Goralski C, Kulas C (2011) Schlanke Fußgängerbrücke aus Textilbeton. *Beton und Stahlbetonbau.* <https://doi.org/10.1002/best.201000081>
7. Büttner T, Orlowsky J, Raupach M (2011) Erhöhung der Dauerhaftigkeit textiler Beton-Bewehrungen durch Epoxidharztränkung. *Bautechnik* 88(5):263–270. <https://doi.org/10.1002/bate.201101460>
8. Offermann P, Engler T, Gries T et al (2004) Technische Textilien zur Bewehrung von Betonbauteilen. *Beton und Stahlbetonbau* 99(6):437–443
9. Quadflieg T, Stolyarov O, Gries T (2016) Influence of the fabric construction parameters and roving type on the tensile property retention of high-performance rovings in warp-knitted reinforced fabrics and cement-based composites. *J Ind Text* 2016:1–19. <https://doi.org/10.1177/1528083716652831>
10. Figueiro R (2011) Fibrous and Composite Materials for Civil Engineering Applications. Woodhead Publishing Limited, Sawston
11. Stolyarov O, Quadflieg T, Gries T (2015) Effects of fabric structures on the tensile properties of warp-knitted fabrics used as concrete reinforcements. *Text Res J* 85(18):1–12. <https://doi.org/10.1177/0040517515578334>
12. Triantafyllou, T., Ed: Textile fibre composites in civil engineering.; Elsevier, 2016, ISBN 9781782424468 .
13. Raof SM, Koutas LN, Bournas DA (2016) Bond between textile-reinforced mortar (TRM) and concrete substrates: Experimental investigation. *Compos B Eng* 98:350–361. <https://doi.org/10.1016/j.compositesb.2016.05.041>
14. Bielak J, Spelter A, Will N et al (2018) Verankerungsverhalten textiler Bewehrungen in dünnen Betonbauteilen. *Beton- und Stahlbetonbau* 113:515–524. <https://doi.org/10.1002/best.201800013>
15. Dilthey, U.; Schleser, M. (2006) Composite improvement of textile reinforced concrete by polymeric impregnation of the textiles; In International Symposium Polymers in Concrete, Guimarães, Portugal, 2 - 4 April 2006. Proceedings of ICPC 2006 / Barroso de Aguiar, J. ; Jalali, S. ; Camoes, A. ; Ferreira, R.M.
16. Reichenbach S, Preinstorfer P, Hammerl M et al (2021) A review on embedded fibre-reinforced polymer reinforcement in structural concrete in Europe. *Construct Build Mater.* <https://doi.org/10.1016/j.conbuildmat.2021.124946>
17. Glowania M, Gries T, Schoene J, Schleser M et al (2011) Innovative Coating Technology for Textile Reinforcements of Concrete Applications. *KEM* 466:167–173. <https://doi.org/10.4028/www.scientific.net/KEM.466.167>
18. Apitzl A, Schmitz J, Hückler A et al (2022) New thermoplastic carbon fiber reinforced polymer rebars and stirrups. *Struct Concrete* 23(2):923–938. <https://doi.org/10.1002/suco.202100434>

19. Alagirusamy R, Barmana KN, Bhattacharya SS (2022) Flexible Towpregs and Thermoplastic Composites for Civil Engineering Applications. In: Alagirusamy R (ed) Flexible Towpregs and Their Thermoplastic. CRC Press, Boca Raton
20. DIN EN ISO 9163 (2005) Textilglas - Rovings - Herstellung von Probekörpern und Bestimmung der Zugfestigkeit von imprägnierten Rovings, DIN Deutsches Institut für Normung e.V.
21. ASTM D 6637 – 01 (2008) Standard Test Method for Determining Tensile Properties of Geogrids by the Single or Multi-Rib Tensile Method, ASTM, 100 Barr Harbor Drive, West Conshohocken

Publisher's Note Springer Nature remains neutral with regard to jurisdictional claims in published maps and institutional affiliations.